A Linear Kronig–Kramers Transform Test for Immittance Data Validation

Bernard A. Boukamp

J. Electrochem. Soc. 1995, Volume 142, Issue 6, Pages 1885-1894.
doi: 10.1149/1.2044210

A Linear Kronig-Kramers Transform Test for Immittance Data Validation

Bernard A. Boukamp*

Department of Chemical Technology, Laboratory of Inorganic Materials Science and Center for Materials Research, University of Twente, 7500 AE Enschede, The Netherlands

ABSTRACT

A method is described with which immittance data can be tested for Kronig-Kramers compliance. In contrast with other procedures, this method is linear in nature and is based on a predetermined set of relaxation times. The model contains as many parameters (or less) as there are data sets. Three modes of operation are described, the first two are based on a linear fit of the model function to the imaginary part or to the real part of the data set. With the fit parameters the corresponding real or imaginary dispersion can be calculated and compared with the actual measurement. In the third mode a complex model function is fitted to the complete data set. As the model function does comply with (a relaxed set of) the Kronig-Kramers (K-K) rules, it will not be able to reproduce the data set satisfactory in the case of nonK-K behavior, as can be observed from the residuals plot. Due to its linear nature, no starting values are needed for the data validation. The main limitation of this procedure is the size of the matrix and the accuracy of the matrix inversion.

Introduction

Electrochemical impedance spectroscopy (EIS) has become an important research tool within the entire electrochemical research community, with significant applications in corrosion research, solid-state electrochemistry, and aqueous and nonaqueous electrochemistry, as well as in electronics. Its application ranges from fundamental investigations to very applied uses such as product quality monitoring. The large advancement in EIS has been brought about by the development of powerful data analysis programs which have become generally available within the last decade. By now the best known and most used programs are LEVM by Macdonald[1-5] and EQUIVALENT CIRCUIT (EQUIVCRT) by the author.[6-8] Both programs are based on a powerful nonlinear least squares fit algorithm developed by Levenberg[9] and Marquardt.[10]

Both complex nonlinear least squares (CNLS) programs are based on the use of an equivalent circuit (EqC) as a modeling function. The nonlinear fit procedure does require an adequate set of starting values for the adjustable parameters of the modeling function. For CNLS-fits with a large number of adjustable parameters, the speed of convergence critically depends on the quality of the starting values. Reasonable values generally can be obtained through graphical means. The software package EQUIVALENT CIRCUIT employs a special subroutine which provides a "rough" deconvolution of the immittance spectra, thus yielding a probable equivalent circuit together with a set of appropriate starting values. This subroutine has the potential for unveiling small contributions to the frequency response that are buried in the overall frequency dispersion.

How well the modeling function reproduces the actual data set can best be observed in a graph of the relative residuals, $\Delta_{re,i}$ and $\Delta_{im,i}$, *vs.* log ω, where ω is the radial frequency ($2\pi f$). The residuals are defined by

$$\Delta_{re,i} = \frac{X_{re,i} - X_{re}(\omega_i)}{|X(\omega_i)|} \text{ and } \Delta_{im,i} = \frac{X_{im,i} - X_{im}(\omega_i)}{|X(\omega_i)|} \qquad [1]$$

with $X_{re,i}$ and $X_{im,i}$ the real and imaginary parts of the ith data set (at frequency ω_i) and $X_{re}(\omega_i)$ and $X_{im}(\omega_i)$ the real and imaginary parts of the modeling function for ω_i. $|X(\omega_i)|$ is the vector length (absolute value) of the modeling function. Besides impedance and admittance, X may also represent the modulus or the dielectric response.

An optimum fit is obtained when the residuals are spread randomly around the log ω axis. When the residuals show a systematic deviation from the horizontal axis, *e.g.*, by forming a "trace" around, above, or below the log ω axis, the CNLS fit is not adequate. This can be caused by several factors, which can be classified into two categories, (*i*) the data contain systematic errors; these can be due to the measuring setup and equipment, aging of the sample, slow change in the sample temperature, *etc.*, and (*ii*) the chosen modeling function is inappropriate; this can be due to a wrong selection and/or arrangement of the dispersive elements, or it may be that the data require a nonideal transfer function (*i.e.*, one that cannot be built up by a set of simple dispersion elements or transfer functions).

It is important to be able to distinguish between cases (*i*) and (*ii*), so that no time is wasted on the interpretation of "bad" data. Here the Kronig-Kramers transforms can be used to indicate whether the data are at fault or the EqC is inadequate. The Kronig-Kramers relations, which are based on the principle of causality,[11-13] dictate that the real and imaginary part of any immittance function are interdependent, provided that the following conditions are met: (*i*) causality: the response must be related to the excitation signal only; (*ii*) linearity: only the first-order term must be present in the response signal. For inherently nonlinear systems (*e.g.*, electrode processes) this implies the use of small excitation voltages, *e.g.* <10 mV; (*iii*) stability: the system may not change with time, nor continue to oscillate when the excitation signal is removed, which requires the system to be passive; and (*iv*) finite: for all values of ω, including $\omega \to 0$ and $\omega \to \infty$.

For practical application of the K-K transforms, this last condition is not critical. The stability condition, however, is the key in the data validation process. The interdependence between the real and imaginary parts of the dispersion is presented in the Kronig-Kramers transform integrals. When the imaginary part of the dispersion is known, the real part can be obtained through the K-K transform integral. In the impedance representation

$$Z_{re}(\omega) = R_\infty + \frac{2}{\pi}\int_0^\infty \frac{xZ_{im}(x) - \omega Z_{im}(\omega)}{x^2 - \omega^2}\,dx \qquad [2]$$

while the imaginary part can be obtained from

$$Z_{im}(\omega) = \frac{2\omega}{\pi}\int_0^\infty \frac{Z_{re}(x) - Z_{re}(\omega)}{x^2 - \omega^2}\,dx \qquad [3]$$

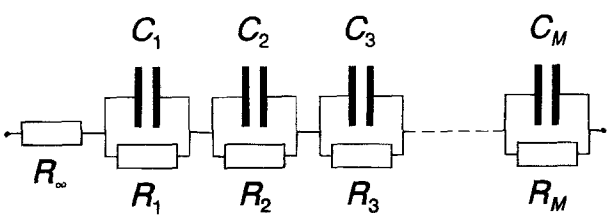

Fig. 1. Equivalent circuit model for the linear Kronig-Kramers transform test of data in the impedance representation.

* Electrochemical Society Active Member.

Thus data from a stable system must comply with these transformation rules. If the imaginary part does not appear to be the same as the real-to-imaginary transform, Eq. 3, or vise versa, then the data set must be considered to be nonK-K transformable, *i.e.*, time varying or nonlinear.

The main problem, however, with applying the K-K transformations is the necessity for integration over the frequency range from 0 to ∞. Several ways have been devised to extend the measured frequency range by extrapolations. Urquidi-Macdonald *et al.*[14] suggested the use of polynomial extrapolation. In a previous publication,[15] extrapolation through the partial fit of a simple circuit (*e.g.*, a resistance in series with a parallel resistance-CPE circuit) was advocated. This works well when the end regions of the frequency dispersion are mainly resulting from a single dispersive function or time constant.

A different approach used by Agarwal *et al.*[16] consisted of modeling the measured impedance data with an EqC represented by a chain of series connected, parallel *R-C* circuits (Voigt circuit, see Fig. 1). As each *R-C* circuit is K-K transformable, the entire circuit must be. Hence if the data can be modeled (within a certain allowable error limit) with this circuit, the data must be K-K transformable. The main advantage is that no extrapolation to zero and infinite frequency is required. The disadvantage of this procedure is that it requires CNLS-fitting and hence a set of starting values. In a recent comparative study by Boukamp and Macdonald,[17] using an improved general multi*R-C* circuit, quite good results were obtained for different data sets. But, as indicated in that study, the calculation procedure is rather time consuming and may require an iterative procedure in which a new *R-C* circuit is added upon a successful convergence until no further improvement is obtained.

A different fit procedure also based on the Voigt circuit of Fig. 1, but linear in its parameters, is presented in this paper. The method of linearization used here is similar to the procedure employed by Uhlman and Hakim.[18] They used it to establish a distribution of relaxation times for a dielectric response. This quite different application is often limited by the occurrence of severe oscillation in the fit parameters as was demonstrated by Morgan and Lesmes.[19] The advantage of these linear procedures, however, is that due to the linear nature no starting values are required and no iterative approximations take place.

With the procedure described in this paper it is possible to perform K-K transformation without the need for evaluation of the Kronig-Kramers integrals and extrapolations to zero and infinite frequency. The applicability and limitations of this procedure are demonstrated on several sets of widely differing dispersion data.

Basic Principle of the Linear Fit

Similarly to the approach presented by Agarwal *et al.*,[16] a chain of parallel *R-C* circuits (Voigt network) is used for data in the impedance representation (see Fig. 1). The imaginary part of the fitting function can then be presented by

$$Z_{im}(\omega_i) = -\sum_{k=1}^{M} \frac{\omega_i R_k^2 C_k}{1 + (\omega_i R_k C_k)^2}$$

$$= -\sum_{k=1}^{M} \frac{\omega_i R_k \tau_k}{1 + (\omega_i \tau_k)^2} \quad \text{with } \tau_k = R_k C_k \quad [4]$$

By taking a fixed distribution for the τ_k,[18] the fit function becomes linear in the R_k values. For M equal to the number of data points, N, a perfect fit can be obtained. This is useful only for near-perfect data; otherwise it would be quite likely that the noise is also (partly) fitted. There are limitless possibilities for the distribution of τ values (time constants, Tcs), but taking the inverse of the measurement frequencies (assuming that these are logarithmically placed along the frequency axis) over the entire frequency range has proved to be an excellent starting point

$$\tau_k = [\omega_k]^{-1} \quad [5]$$

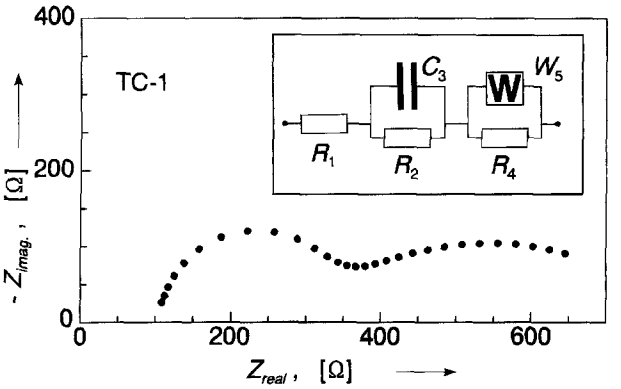

Fig. 2. Impedance representation of the dispersion of test circuit 1 (TC-1). The equivalent circuit is represented in the inset. Parameter values are given in Table I. The frequency range is 1 Hz to 10 kHz with seven points/decade.

For simplicity and demonstration purposes we take the number of adjustable parameters, M, equal to the number of data sets, N. The results in M simultaneous equations of the type of Eq. 4. Hence by using a single-matrix inversion or matrix solving routine the set of R_k values is obtained. Due to the size of M, the matrix routine must have high precision. For the results that will follow a Gauss-Jordan pivoting routine,[20] implemented in Turbo Pascal (®Borland International), has been employed successfully.

The basic assumption in the approach is that the above fitting function smoothly follows the imaginary data set ($Z_{im,i}$ *vs.* log ω). As the fit function is *a priori* K-K transformable, its real part, which is calculated directly from the parameter set, might be expected to follow the real data set, provided that the data set complies with the K-K transformation rules. The real part of the fitting function is simply given by

$$Z_{re}(\omega_i) = R_\infty + \sum_{k=1}^{M} \frac{R_k}{1 + (\omega_i \tau_k)^2} \quad [6]$$

R_∞ is the high (infinite) frequency cutoff resistance which cannot be obtained from the K-K transform of the imaginary data set. Its value can quite simply be determined by calculating the mean distance between the actual real data set and the transformed set.[15] In case of a large variation in the impedance vector length over the frequency range it is necessary to calculate the weighted mean for R_∞

$$R_\infty = \frac{\sum_{i=1}^{N} w_i \left[Z_{re,i} - \sum_{k=1}^{M} \frac{R_k}{1 + (\omega_i \tau_k)^2} \right]}{\sum_{i-1}^{N} w_i} \quad [7]$$

(the weight factor, w_i, is defined below). To demonstrate this procedure, a simple data file is simulated using the test circuit presented in the inset in Fig. 2 (denoted further on as TC-1). The frequency range and selected parameters are given in Table I. The data file, which was obtained through the simulation subroutine of EQUIVALENT CIRCUIT, does not extend to the real axis at either frequency limit. For a proper K-K transform using the integrals of Eq. 1 and 2, an extrapolation is definitely necessary.[15] The model function, Eq. 4, was fitted exactly to the imaginary part of this data

Table I. Parameter values for the elements of the test circuit of Fig. 2. The W symbol represents a Warburg type response: $Z(\omega) = [Y_0 \sqrt{j\omega}]^{-1}$. The frequency range was 1 Hz to 10 kHz with seven points/decade (29 data points).

Element/parameter	Value	Unit
R-1	100	Ω
R-2	200	Ω
C-3	0.8	μF
R-4	500	Ω
W-5, Y_0	4×10^{-4}	$S.s^{0.5}$

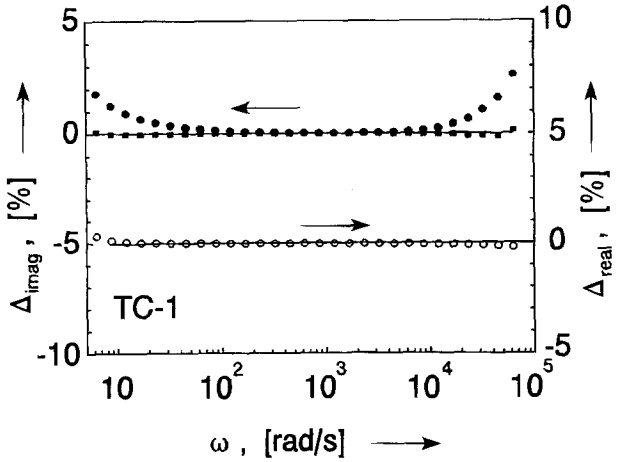

Fig. 3. Relative deviations between the measured and K-K transform calculated dispersion. Lower part, right axis, (○) $\Delta_{re,i}$, K-K transform of imaginary fit (Eq. 4). Upper part (left axis) $\Delta_{im,i}$, (●) K-K transform of real fit (Eq. 8) and (■) K-K transform of real fit followed by adjustment using Eq. 10.

set (TC-1). The residual relative error between the K-K transform and the real part of the dispersion is presented in the lower part of Fig. 3 (open circles). The deviation between the transformed set and the real data set is less than 0.4% and is most pronounced at both ends of the frequency range.

Similarly we can fit the model function to the real part of the dispersion, but here R_∞ must be included as fit parameter (R_∞ is represented by R_1)

$$Z_{re,i} = R_1 + \sum_{k=2}^{M} \frac{R_k}{1 + (\omega_i \tau_k)^2} \qquad [8]$$

Of course, R_1 does not appear in the imaginary transform. The result of the real fit and transformation to the imaginary part is also presented in Fig. 3 (upper part, closed circles). Here a relatively large deviation is observed at both ends of the frequency dispersion (~3%). Apparently the information contained in the real part of the dispersion is insufficient to construct accurately the imaginary part. It may be assumed that other fit models will result in different transformations to the imaginary part of the dispersion, despite the fact that the real part fits (within the error of the calculation) are virtually indistinguishable. In other words: although no extrapolation of the fit function is made visible in this procedure, it is implied in the transformation to the imaginary part. The implication of this is that the precision, with which the imaginary part can be extracted from the real part of the dispersion, depends critically on the extent of the frequency range employed. Hence, increasing the frequency range is expected to yield

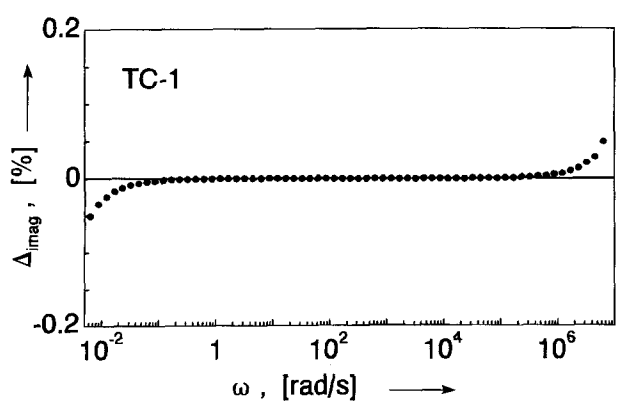

Fig. 4. Relative imaginary deviation, $\Delta_{im,i}$, obtained for the K-K transformation of the real part fit (Eq. 8), without adjustment, for the extended (1 mHz to 1 MHz) dispersion data of test circuit TC-1 (inset Fig. 2). Note the difference in the vertical scale with respect to Fig. 3.

a significant improvement, which is demonstrated in the imaginary residual plot of Fig. 4. Here the frequency range for TC-1 (Fig. 2, Table I) was increased from 4 decades to 9 decades (1 mHz to 1 MHz). Now the relative deviation for the real to imaginary transformation, $\Delta_{im,i}$, is 0.05% at most at both ends of the frequency spectrum, which represents an excellent fit.

On the other hand it can be argued that the model function for the real part of the dispersion cannot contain elements which give only a contribution to the imaginary part. In the impedance representation these can be a capacitance and an inductance in series with the equivalent circuit of Fig. 1. In fact, this assumption does suggest that the real to imaginary K-K transform could be augmented to

$$Z_{im}(\omega) = \omega L - (\omega C)^{-1} + \frac{2\omega}{\pi} \int_0^\infty \frac{Z_{re}(x) - Z_{re}(\omega)}{x^2 - \omega^2}\, dx \qquad [9]$$

which could be viewed as a "relaxed form" of the K-K transformation. But some caution must be exercised here. The K-K transform integral (Eq. 2) yields zero for a series capacitance ($Z_{im} = -1/\omega C$), thus not giving a direct violation. For a series inductance, however, the integral goes to infinity. Unless the inductance is bypassed by a circuit (*e.g.*, resistance) which will cause the high frequency dispersion to return to the real axis for $\omega \to \infty$, Eq. 9 is not valid. For the limited frequency ranges used in this study, however, this limitation can be ignored without consequences.

Hence, after the transformation of the real part to yield the calculated imaginary part, $Z_{im}(\omega_i)$, a second linear fit procedure is performed with the series inductance and capacitance as adjustable parameters

$$S = \sum_{i=1}^{N} w_i \left[Z_{im,i} - Z_{im}(\omega_i) - L\omega + X/\omega \right]^2 \qquad [10]$$

where $X = 1/C$. By setting $\partial S/\partial L$ and $\partial S/\partial X = 0$, the L and X values can be obtained from the resulting matrix equations. The result of this second operation is also presented in Fig. 3 (upper part, solid squares), indicating a significantly improved fit. Thus, although the imaginary part of the dispersion cannot be retrieved with precision for data with a limited frequency range, it is still possible to check whether, or not, this data set obeys the K-K transformation rules. This is done by comparing the transformed and adjusted (Eq. 7 and 10) fit functions to the actual data. If data do not comply with K-K, Eq. 6-10 will not lead to a random distribution of the residuals along the log ω axis.

But when the intention is just to check the data for K-K compliance, it is far more appropriate to fit the complex transform function to the complete data set by minimizing the following error sum

$$s = \sum_{i=1}^{N} w_i \left(\left[Z_{re,i} - R_1 - \sum_{k=3}^{M-1} \frac{R_k}{1 + (\omega_i \tau_k)^2} \right]^2 + \left[Z_{im,i} + \frac{X_2}{\omega_i} + L_M \omega_i - \sum_{k=3}^{M-1} \frac{R_k \omega_i \tau_k}{1 + (\omega_i \tau_k)^2} \right]^2 \right) \qquad [11]$$

where X_2 (=$1/C = R_2$) is the second fit parameter and L_M is the last fit parameter (=R_M). Hence, the fit parameters R_k may have different dimensions. Taking $\partial S/\partial R_q = 0$ yields M linear simultaneous equations

$$q = 1 \quad \sum_{i=1}^{N} w_i Z_{re,i} = \sum_{i=1}^{N} w_i \left[R_1 + \sum_{k=3}^{M-1} \frac{R_k}{1 + (\omega_i \tau_k)^2} \right]$$

$$q = 2 \quad \sum_{i=1}^{N} w_i \frac{Z_{im,i}}{\omega_i} = \sum_{i=1}^{N} w_i \left[-\frac{X_2}{\omega_i^2} + L_M - \sum_{k=3}^{M-1} \frac{R_k \tau_k}{1 + (\omega_i \tau_k)^2} \right]$$

$$2 < q < M \quad \sum_{i=1}^{N} w_i \frac{Z_{re,i} + Z_{im,i} \omega_i \tau_q}{1 + (\omega_i \tau_q)^2} = \sum_{i=1}^{N} \frac{w_i}{1 + (\omega_i \tau_q)^2} \left[R_1 - X_2 \tau_q + L_M \omega_i^2 \tau_q + \sum_{k=3}^{M-1} R_k \frac{1 - \omega_i^2 \tau_k \tau_q}{1 + (\omega_i \tau_k)^2} \right]$$

$$q = M \quad \sum_{i=1}^{N} w_i Z_{im,i} \omega_i = \sum_{i=1}^{N} w_i \left[-X_2 + L_M \omega_i^2 - \sum_{k=3}^{M-1} \frac{R_k \omega_i^2 \tau_k}{1 + (\omega_i \tau_k)^2} \right] \qquad [12]$$

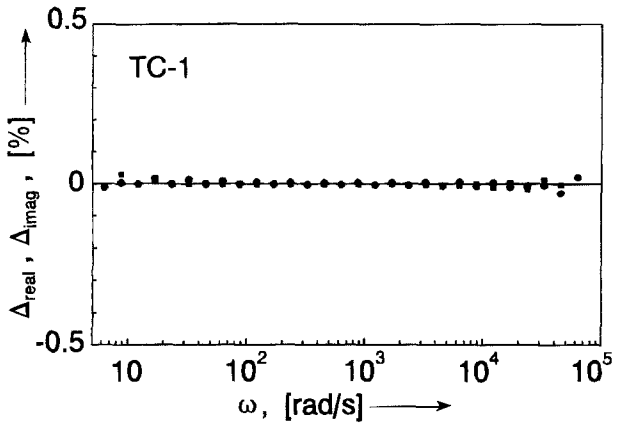

Fig. 5. Relative deviations, $\Delta_{re,i}$ (●) and $\Delta_{im,i}$ (■) for the complex linear fit of the TC-1 impedance data (Fig. 2) using Eq. 11.

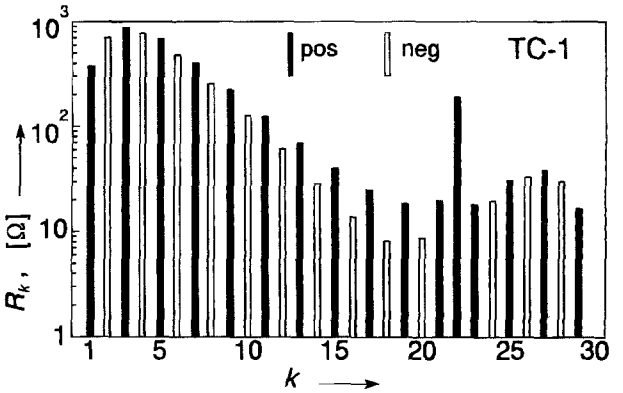

Fig. 6. Distribution of the R_k values for the imaginary fit to the simulated TC-1 impedance data (Fig. 2). Positive values are indicated by the filled bars, negative values by the open bars.

The weight factor, w_i, is taken as

$$w_i = [(Z_{re,i})^2 + (Z_{im,i})^2]^{-1} \quad [13]$$

under the assumption that the random noise present in the data originates before the signal is split into a real and imaginary part and that its magnitude, in first approximation, is proportional to the absolute value of the impedance vector length (see also Ref. 7 and 21). This assumption is generally fulfilled as can be seen from the following examples.

The set of M simultaneous equations (Eq. 12) is again solved using standard matrix inversion techniques (Gauss-Jordan[20]). As there are in principle more data points ($2N$, a real and an imaginary set) than adjustable parameters, this fit procedure should not result in a "perfect fit " for $M = N$, as was possible for the single real and imaginary fits. Although, depending on the data, M could be taken larger then N, this has no real advantage as will be demonstrated below. An example of this complex fit performed on the TC-1 data set is presented in the residuals plot of Fig. 5. The range of the vertical axis is a factor of 10 smaller than in the plot of the residuals for the solitary transforms (Fig. 3), indicating an excellent fit. That the fit is not "perfect" is demonstrated by the pseudo chi-squared fit value, $\chi^2_{ps} = 7.6 \times 10^{-8}$, where χ^2_{ps} is defined here by

$$\chi^2_{ps} = \sum_{i=1}^{N} w_i ([Z_{re,i} - Z_{re}(\omega_i)]^2 + [Z_{im,i} - Z_{im}(\omega_i)^2]) \quad [14]$$

Hence, for randomly distributed relative residuals, the mean value is approximately equal to the square root of χ^2_{ps}, *i.e.*, a mean error of 0.5% for $\chi^2_{ps} = 2.5 \times 10^{-5}$. From Fig. 5 it is clear that with this linear modeling function an excellent fit to the data can be obtained, and that in a much shorter time than with either the model presented by Agarwal *et al.*[16] or the models presented by Boukamp and Macdonald.[17]

The Fitted Parameter Set

So far no attention has been paid to the appearance of the thus calculated parameter set, R_k. As no restrictions are placed on the values the R_k may attain, negative values also belong to the possibilities. In fact, it turns out that the R_k values are almost alternatingly positive and negative, which is generally endemic to this class of fit procedures.[19] An example of the parameter values obtained for the imaginary fit of the test circuit of Fig. 2 is presented in Fig. 6 and clearly shows the alternating sign. As the τ values are by definition positive, the corresponding capacitances have the same sign as the resistances. Hence double negative parallel R-C pairs are formed, which present a semicircle below the real axis (taking $-Z_{im}$ as positive y-axis) in the impedance representation. These negative R-C pairs, which also obey the K-K rules, might be interpreted as "corrections" on the contribution of the positive R-C pairs.

But now the question arises whether the fit model functions behave smoothly between the original data points. That this is the case (at least for the ideal data set of TC-1, Fig. 2) is demonstrated in Fig. 7 where both the real (Eq. 8) and imaginary (Eq. 4) model functions are evaluated at four additional intermediate frequency points between each pair of original frequency values. Hence it may be concluded that this oscillatory behavior has no consequences for the fit procedures presented here. But it also means that no physical meaning may be attributed to the obtained fit parameters.

It turns out that for immittance data which contain little random noise (*e.g.*, <0.5% of $|Z_i|$) a perfect fit is obtained in the primary (real *c.q.* imaginary) data set, while the relative residuals (Eq. 1) of the transformed pairs are increased with respect to the error distribution in the complex fit of Eq. 1.

Influence of the *M*-*N* Ratio and Noise

As indicated above, even when data contain noise, they can be fitted perfectly in the single part mode using Eq. 8 for the real part fit and Eq. 4 for the imaginary part fit. But it is possible to average the noise by just reducing the number of parameters, M, with respect to the number of data sets, N (which effectively means a reduction in the number of Tcs per decade). For the single real and imaginary fit this requires minimization of an error sum by setting its partial derivatives to zero, similar to the complex fit procedure of Eq. 11. The error sum for the real part fit is then given by

$$S = \sum_{i=1}^{N} w_i \left[Z_{re,i} - R_1 - \sum_{k=2}^{M} \frac{R_k}{1 + (\omega_i \tau_k)^2} \right]^2 \quad [15]$$

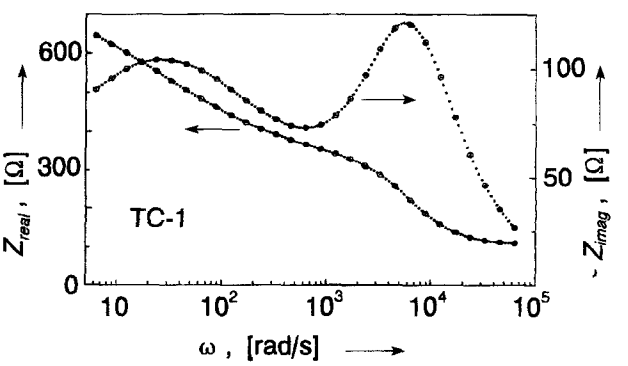

Fig. 7. Comparison between the TC-1 impedance data and the fit model functions. Left axis for the real data and real fit function (Eq. 8), right axis for the imaginary data and imaginary fit function (Eq. 4). Data points are indicated by (○). The fit function values are calculated at four extra frequencies between each original frequency pair and are presented by (•).

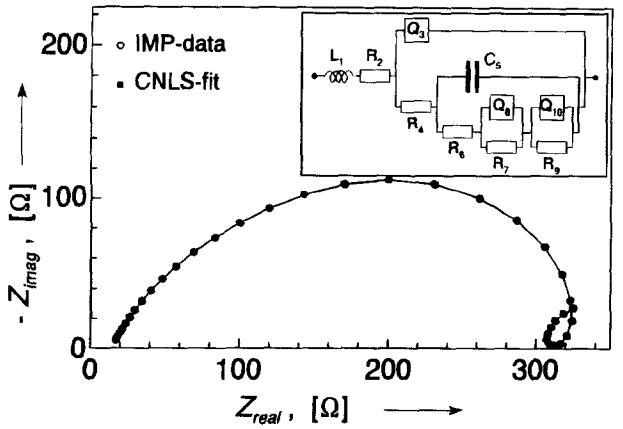

Fig. 8. Impedance representation of the dispersion data of the Fe-implanted, yttria-stabilized zirconia/gold, oxygen electrode (IMP).[8] (○) Actual measurements, (■) fit function dispersion. The fit function parameters are presented in Table II. The EqC used in the CNLS-fit is presented in the inset.

Setting the $\partial S/\partial R_q$ equal to zero again yields M simultaneous equations, linear in the parameters R_q

$$q = 1 \quad \sum_{i=1}^{N} w_i Z_{re,i} = \sum_{i=1}^{N} w_i \left[R_1 + \sum_{k=1}^{M} \frac{R_k}{1 + (\omega_i \tau_k)^2} \right]$$

$$q > 1 \quad \sum_{i=1}^{N} w_i \frac{Z_{re,i}}{1 + (\omega_i \tau_q)^2} = \sum_{i=1}^{N} w_i \left[R_1 + \sum_{k=1}^{M} \frac{R_k}{1 + (\omega_i \tau_k)^2} \right] \frac{1}{1 + (\omega_i \tau_q)^2} \quad [16]$$

The τ values are taken to span the entire frequency region. Consequently Eq. 3 must be adjusted accordingly

$$\tau_k = \tau_1 \exp\left[\frac{k-1}{M-1} \ln \frac{\tau_M}{\tau_1} \right]$$

$$\text{with } \tau_1 = [\omega_1]^{-1} \text{ and } \tau_M = [\omega_N]^{-1} \quad [17]$$

which yields a series of τ values spaced at equal intervals along the log τ axis ($-\log \omega$ axis). Applying the Gauss-Jordan routine yields the fit function parameters, R_k. To demonstrate the influence of the M/N ratio on the fit quality, a different set of impedance data is analyzed. This data set (denoted IMP) was obtained for an O_2,Au/Fe-implanted yttria-stabilized zirconia electrode. A CNLS-fit analysis of the IMP-data set, using EQUIVALENT CIRCUIT, has been presented in Ref. 8 and is shown in Fig. 8. This impedance data has also been successfully subjected to a K-K transform test using a nonlinear set of R-C circuits, as well as to a full K-K transformation using end-region extrapolation.[15] Results have been published recently by Boukamp and Macdonald.[17]

The dependence of χ^2_{ps} on the M/N ratio for this data set is presented in Fig. 9. The complex fit (Eq. 11) shows more or less a plateau at $\chi^2_{ps} = 1.2$ to 1.4×10^{-6} above $M/N = 0.9$. The real part fit (Eq. 15) is much less sensitive to the M/N ratio, but shows a much higher χ^2_{ps} value (2×10^{-5} to 3×10^{-5}). The weighted imaginary part fit (equations not presented) gave a somewhat more complicated picture. The lowest value for χ^2_{ps} (2.5×10^{-6}) was observed in the range $0.65 < M/N < 0.85$. A similar plot for the complex fit of the (ideal) TC-1 data gave an almost exponential dependence for χ^2_{ps} ranging from $\chi^2_{ps} = 7.6 \times 10^{-8}$ for $M/N = 1$ to 3.8×10^{-5} for $M/N = 0.5$. Comparing this behavior with the complex fit of Fig. 9 suggests that the plateau in Fig. 9 results from the noise present in the data. The residuals plot of $M/N = 1$ for the complex linear fit is identical in appearance to the residual plot for the CNLS fit of the IMP-data (Table II). The χ^2_{ps} values are also close: 1.2×10^{-6} for the complex linear fit with $M = N$ *vs.* 4.4×10^{-6} for the CNLS-fit (EQUIVCRT).

Influence of the τ Range

Besides the N/M ratio we can also vary the range of τ values. So far the range has been set equal to the range of inverse frequencies (Eq. 5 or 17). This τ range can be enlarged, thus including RC-time constants which lie outside the measured frequency range. Again it is useful to monitor the pseudo χ^2 values obtained in the linear fit procedures. For testing purposes both the lower τ limit and the upper τ limit have been shifted by the same amount. For demonstration purposes we start with a τ range smaller than the range of frequencies, varying the extension factor, F_{ext}, from 0.125 to about 10^6 in a factor of two increments, with

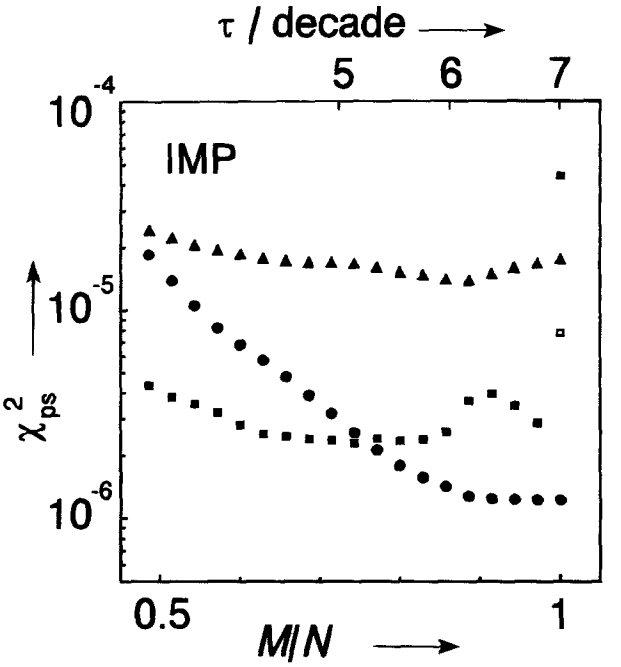

Fig. 9. Influence of the M/N ratio on χ^2_{ps} in the weighted fit procedures applied to the IMP data: (●) for the complex fit, Eq. 11; (■) for the real part fit with imaginary adjustment (in analogy with Eq. 15 and using subsequently Eq. 10); (▲) for the imaginary part fit, Eq. 15. The (□) indicates the χ^2_{ps} for the unweighted fit according to Eq. 4. The unweighted real fit (Eq. 8 and 10) yielded the same χ^2_{ps} as the weighted fit for M/N. The top axis represents the resulting number of Tcs per decade.

$$\tau_1 = \frac{F_{ext}}{\omega_1} \quad \tau_M = \frac{1}{F_{ext}\omega_n} \quad [18]$$

and calculating the τ_k using Eq. 17.

The influence of the τ range on χ^2_{ps} for the IMP data, with $M = N$, is presented in Fig. 10. Both the real part (solid squares) and imaginary part (solid triangles) fit procedures are extremely sensitive to deviations from the previously defined τ range. Although the primary fit to the partial dispersions is quite good ($\chi^2_{ps} \sim 10^{-7}$), the transforms show a large deviation for $F_{ext} < 0.5$ or $F_{ext} > 2$. A sharp

Table II. Parameter values and error estimates for the EqC (inset Fig. 8) used in the CNLS fit of the Fe-implanted electrode data "IMP".[8] The fit yielded $\chi^2_{ps} = 4.4 \times 10^{-6}$ using function proportional weighting. The Q symbol represents a constant-phase element (CPE) with the admittance representation: $Y(\omega) = Y_0 (j\omega)^n$.

Element/parameter		Value	Rel. error (%)	Unit
L_1		2.02×10^{-5}	3	H
R_2		13.4	0.5	Ω
Q_3	Y_0	5.05×10^{-5}	2	$S.s^n$
	n	0.695	0.4	—
R_4		311	2	Ω
C_5		3.6×10^{-5}	10	F
R_6		57	7	Ω
R_7		−86	9	Ω
Q_8	Y_0	-8.7×10^{-4}	5	$S.s^n$
	n	0.83	3	
R_9		88	23	Ω
Q_{10}	Y_0	1.7×10^{-2}	14	$S.s^n$
	n	0.79	13	

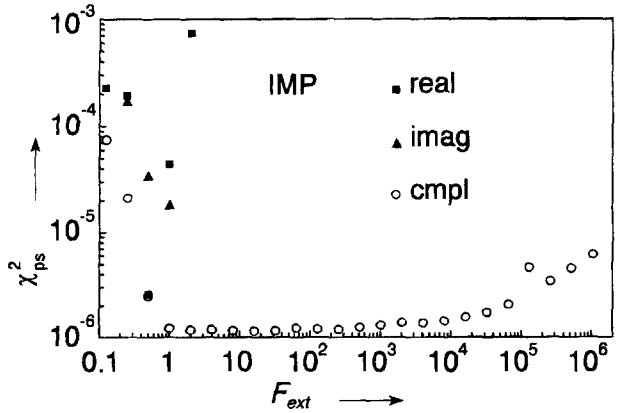

Fig. 10. Influence of the τ range on χ^2_{ps} for the IMP data set: (○) complex fit procedure using Eq. 11 with *M/N*, (■) the weighted real part fit (Eq. 15), and (▲) the weighted imaginary part fit.

minimum is located at F_{ext} = 0.5 to 1, which is quite an unexpected result.

In contrast, in the complex fit the τ range can be extended on both sides over a large number of decades without a significant increase in χ^2_{ps} (Fig. 10, open circles). Over this range of τ extensions, the number of negative *R-C* pairs in the complex fit function does decrease to some extent, although in a rather erratic fashion. Changing the *M/N* ratio shifts the upturn in χ^2_{ps} to lower F_{ext} values (from about 10^4 for $M = N = 35$ to 10^3 for $M = 30$).

Test of NonK-K Transformable Data

Besides showing that this fit/transform procedure works well for simulated and for properly measured data, it is important to demonstrate its power to unveil data that is not compliant with the K-K transformation. To illustrate this, an impedance data set of terbium-doped yttria-stabilized zirconia (TZY), which has also been tested for K-K compliance in Ref. 17, is analyzed here. The original measurements were performed in a nitrogen atmosphere. Apparently the mixed conducting sample was not in thermodynamic equilibrium with the oxygen partial pressure in the ambient ($pO_2 \approx 10^{-4}$ atm) during the impedance measurement. Hence, it is assumed that oxygen continued to diffuse out of the sample, thus increasing the electronic conductivity during the measurement sequence and hence causing a distortion of the impedance spectrum. The measured dispersion and the best CNLS fit simulation are presented in the impedance representation in Fig. 11. The EqC used is shown in the inset of Fig. 11. The measurements were performed at 10.5 frequency points per decade. Hence

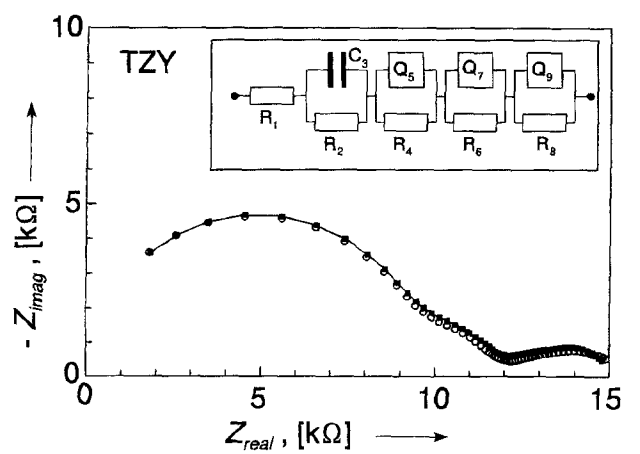

Fig. 11. Impedance representation of the dispersion data of the terbium-doped YSZ sample (TZY).[17] (○) Actual measurements, (■) fit function dispersion. The EqC used in the fit is presented in the insert.

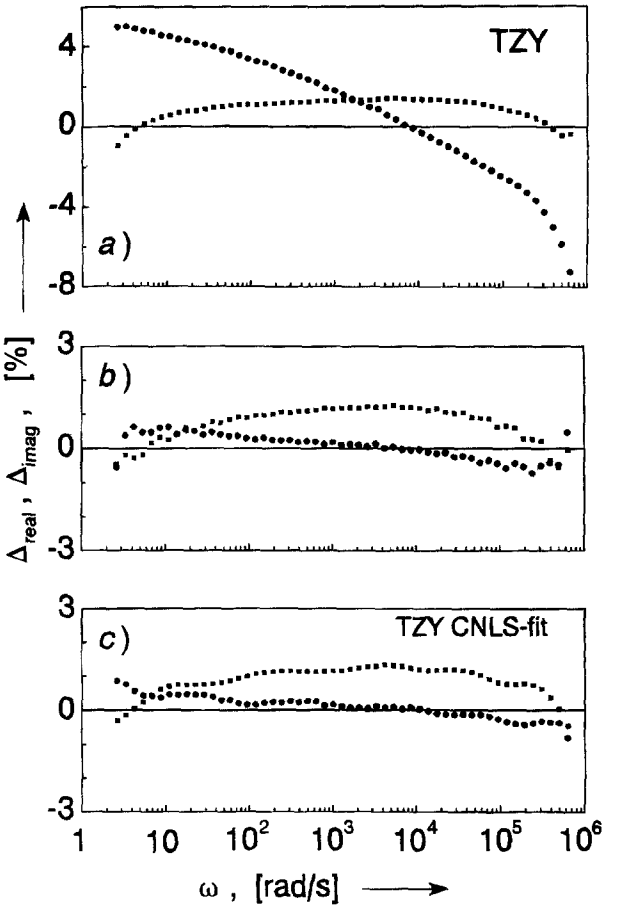

Fig. 12. Residuals plot for the fit transforms of the TZY impedance data which shows nonK-K behavior. Presented are the relative errors, $\Delta_{re,i}$ and $\Delta_{im,i}$, (a) for the real-to-imaginary transformation (○) and for the imaginary-to-real transformation (□), (b) for the complex transformation (Eq. 11) and (c) for the CNLS-fit. (●) = $\Delta_{re,i}$, (■) = $\Delta_{im,i}$.

the number of fit variables, *M*, was substantially reduced to 40 (~eight τ values per decade, number of data points N = 53). In Fig. 12 the residuals plots are presented for the separate real and imaginary (adjusted) transform fits (Fig. 12a) and the complex function fit (Fig. 12b), while the residuals of the CNLS-fit are presented in the lower part.

It is evident from this figure that the single transforms are very sensitive to nonK-K behavior. Especially the real-to-imaginary transform shows a distinct deviation from the zero error axis. As the complex fit function (Eq. 11) tries to accommodate both parts of the data set, the deviation from ideal behavior is less pronounced, but the clear trace above and below the zero error axis is still a prominent indication that the data do not comply with the K-K transform rules. The form of this residuals plot is very much like the CNLS-fit residuals plot (Fig. 12c), as are the χ^2_{ps} values: 0.9×10^{-4} for the complex linear fit (Eq. 11) and 1.4×10^{-4} for the CNLS-fit. This can be taken as an indication that the EqC of Fig. 11 represents one of the closest fits to this flawed data set. An interesting observation for this data set is that the χ^2_{ps} values were quite insensitive to variation of the *M/N* ratio in the range 0.4 to 1, with χ^2_{ps} about 10^{-4} for the complex and real part fit, and $\chi^2_{ps} \sim 10^{-3}$ for the imaginary part fit.

Systems with Blocking Electrodes

The impedance spectra of samples with "blocking" electrodes seem to pose a problem for the K-K transformation as they do not appear to be finite for $\omega \to 0$ (*i.e.*, not returning to the real axis). Of course for very low frequencies the overall electronic resistance, how ever large it may be, will dominate the impedance spectrum and cause a, generally very large, finite dc-resistance for $\omega \to 0$. But this will take effect only for impractically low frequencies. When the

high frequency resistance has a finite value, the easiest way is to transform the impedance data to the admittance representation where the blocking electrode dispersion will yield a low frequency semicircle which passes through the origin.

In analogy with the chain of parallel *R-C* circuits (Fig. 1) a ladder of series *R-C* circuits (Maxwell circuit model), as presented in Fig. 13, can be envisioned as basis for the fit function. In order to compensate for the nontransforming "capacitive and inductive" offset in the imaginary part of the dispersion (compare Eq. 11) also a parallel capacitance and inductance have been added to the circuit of Fig. 13. With this again a linear fit function can be formulated, now with C_k as adjustable parameter set

$$Y(\omega_i) = \frac{1}{R_1} + \sum_{k=3}^{M-1} \frac{C_k\omega_i^2\tau_k}{1+(\omega_i\tau_k)^2} + j\left[C_2\omega_i - \frac{1}{L_M\omega_i} + \sum_{k=3}^{M-1} \frac{C_k\omega_i}{1+(\omega_i\tau_k)^2}\right] \quad [19]$$

with $C_1 = 1/R_1$ and $C_M = 1/L_M$. To test the validity of this linear fit procedure a published set of admittance data, obtained for a single crystal of Li_3N with blocking gold electrodes,[22] has been used. This data set (hereafter named Li3N) has been subjected to a comprehensive CNLS data analysis which has been published recently by Macdonald.[23] In Fig. 14 both the impedance and the admittance representations of the Li3N dispersion are presented together with the simulations of a CNLS-fit using the EQUIVALENT CIRCUIT package. The EqC used in this fit is presented in the inset of Fig. 14a; the associated parameter values are given in Table III. This EqC, which gave a χ^2_{ps} value of 8.3×10^{-6} for function proportional weighting, is different from the one presented by Macdonald.[23] It is not necessarily the most physically realistic model; it just serves our purpose of comparing the best CNLS fit with the linear model transform. Similarly to the analysis of the

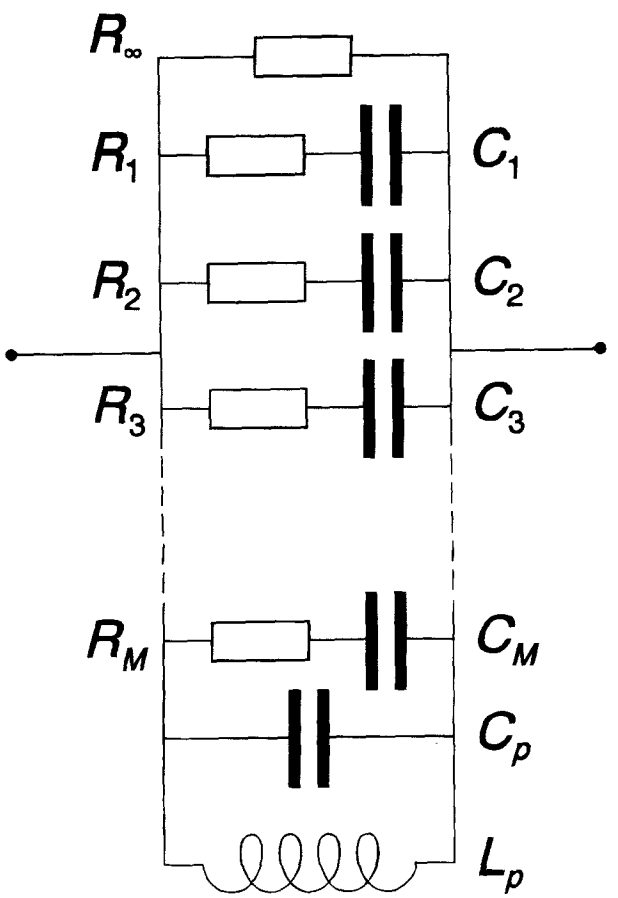

Fig. 13. Schematic representation of the equivalent circuit which is used in the linear transformation/fit procedure of admittance data.

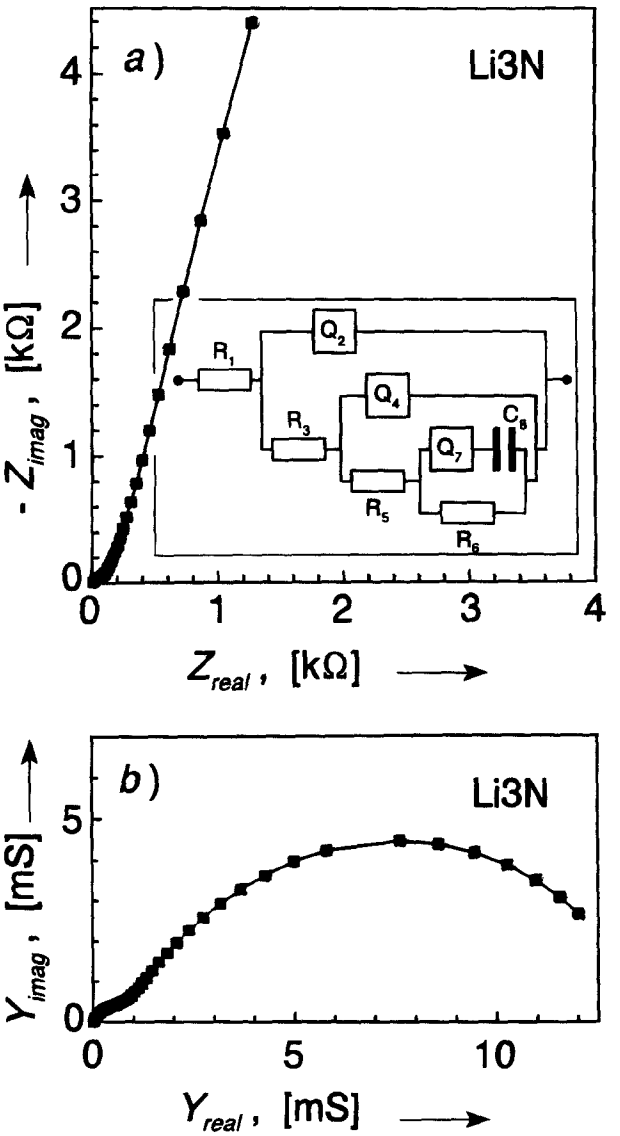

Fig. 14. Presentation of the dispersion measured for a hydrogen doped Li_3N single crystal with gold electrodes at 45°C, according to Ref. 23. (a) Impedance representation, (b) admittance representation. (○) measured data, (■) CNLS-fit result (see Table III). The EqC used in the CNLS-fit is presented in the inset of Fig. 14a.

IMP data, first the dependence of χ^2_{ps} on the *M/N* ratio, *i.e.*, th number of Tcs per decade, was investigated. The results are presented in Fig. 15. Clearly the best results for the partial fit and transform procedures are obtained with less than 7 Tcs per decade, while the complex lineary fit (Eq. 19) is found to be much less sensitive to this parameter. A comparison of the corresponding residuals plots for $M = 35$ is

Table III. Parameter values and error estimates for the EqC used in the CNLS fit of the Li3N data.[23] The fit yielded $\chi^2_{ps} = 8.3 \times 10^{-6}$ using function proportional weighting. See caption Table II for the definition of the Q element.

Element/parameter		Value	Rel. error (%)	Unit
R_1		73.5	0.5	Ω
Q_2	Y_0	4.0×10^{-7}	17	$S.s^n$
	n	0.822	1.5	—
R_3		430	17	Ω
Q_4	Y_0	7.2×10^{-7}	30	$S.s^n$
	n	0.76	4	
R_5		600	11	Ω
R_6		8.2×10^5	14	Ω
Q_7	Y_0	2.17×10^{-5}	4	$S.s^n$
	n	0.566	1	
C_8		3.52×10^{-6}	4	F

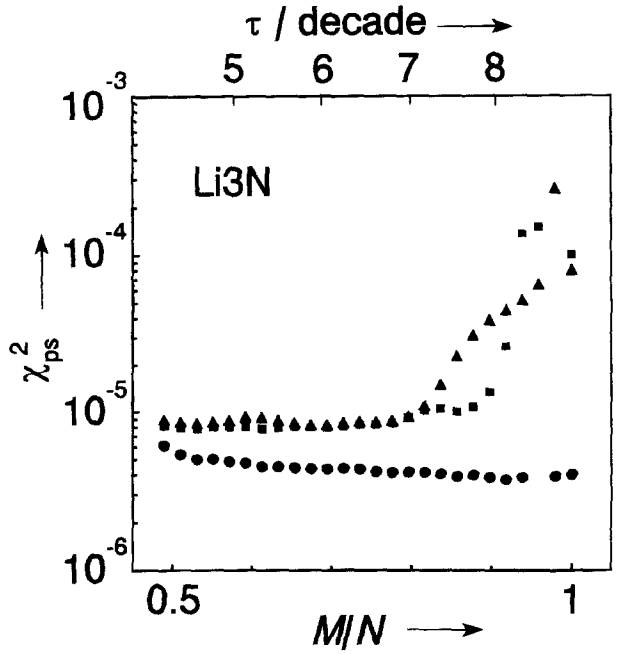

Fig. 15. Influence of the *M/N* ratio on χ^2_{ps} in the weighted admittance fit procedures applied to the Li3N data: (●) for the complex fit, Eq. 19; (■) for the weighted real part fit with imaginary adjustment, (▲) for the weighted imaginary part fit. The top axis represents the resulting number of Tcs per decade.

presented in Fig. 16 for the real to imaginary transform (top section), the imaginary to real transform (middle section), and the complex linear fit (bottom section). Especially for the complex fit a very good χ^2_{ps} value of 4.4×10^{-6} is obtained. In the real to imaginary part transform, the subsequent parallel C and L adjustment (cf. Eq. 10) was included. Without this adjustment, a rather poor fit was obtained, indicating that reconstruction of the imaginary dispersion from the real part cannot be done with precision for this data set.

When the impedance dispersion of a system with blocking electrodes includes the bulk (dielectric) response, a shift to the admittance plane is not useful since the dielectric part will present a straight line for $\omega \rightarrow \infty$ in the admittance representation. This problem has been recognized by Láng *et al.*[24] Their approach, which is also applicable in this context, is to add mathematically a sufficiently small parallel resistance value to the measured dispersion. This will result in a downward curving of the electrode response, and thus allows analysis with the linear fit functions of Eq. 4-10 in the impedance representation. Conversely one could also add a series resistance to the dispersion data and subsequently perform the analysis in the admittance representation. In the next paragraph, an example is presented of the application of this modified dispersion procedure to

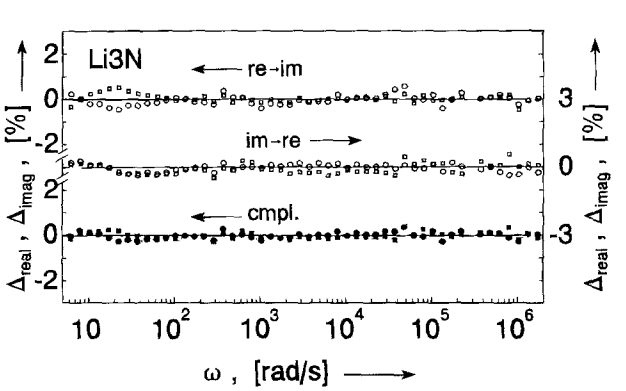

Fig. 16. Residuals plot for the complex linear fit of the Li3N data set with *M* = 35 (~6.2 τ values per decade).

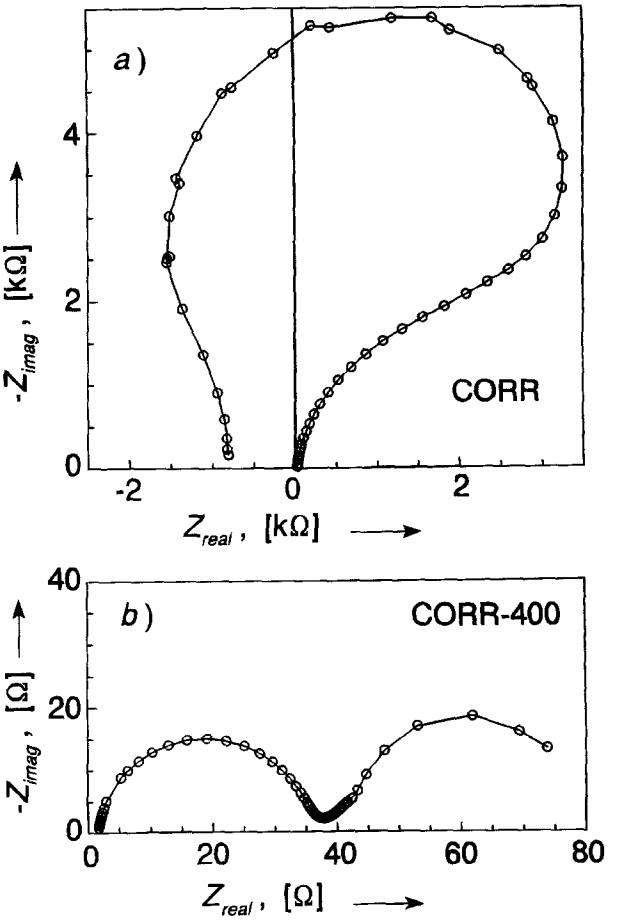

Fig. 17. Impedance representation of the dispersion of a corroding Cr electrode in 0.5*M* sulfuric acid at −0.95 V *vs.* a saturated mercurous sulfate electrode (active-passive transition region). (a) Actual impedance data CORR according to Ref. 25-27, (b) impedance data after computational addition of a parallel resistance of 400 Ω, denoted by CORR-400.

impedance data which present a different problem for K-K validation.

Data Validation of Dispersions with a Negative Resistance

A special group is formed by impedance data which includes a single negative resistance. This phenomenon is mostly observed in corrosion studies. The negative differential resistance is a direct consequence of the negative slope in the current/polarization curve just above the passivation voltage.[25] In principle this group of data cannot be checked for validity by the K-K transformation as was demonstrated by Urquidi-Macdonald *et al.*[14] There is, however, a simple way to resolve this problem by adding a small enough parallel resistance to the dispersion data so that the negative resistance is removed completely. This procedure, which is entirely compatible with the K-K transform rules, is similar to the alternative method proposed for the impedance data of blocking electrodes.[24] As an example a typical impedance data set (CORR) is used which was obtained for pure chromium in 0.5*M* sulfuric acid in the active-passive transition region (courtesy of Dr. J. A. L. Dobbelaar, Fig. 17a). It was the first time that this type of dispersion data was completely resolved by CNLS fitting.[25-27] From the dispersion presented in Fig. 17a it can be estimated that adding a parallel resistance of 400 Ω is sufficient to eliminate the negative resistance and to shift the impedance dispersion to the second quadrant of the complex plane, which then takes the form as presented in Fig. 17b. This data set, named CORR-400, contained 62 data points over a frequency range of about 6.4 decades. Hence first the relation between χ^2_{ps} and the *M/N* ratio

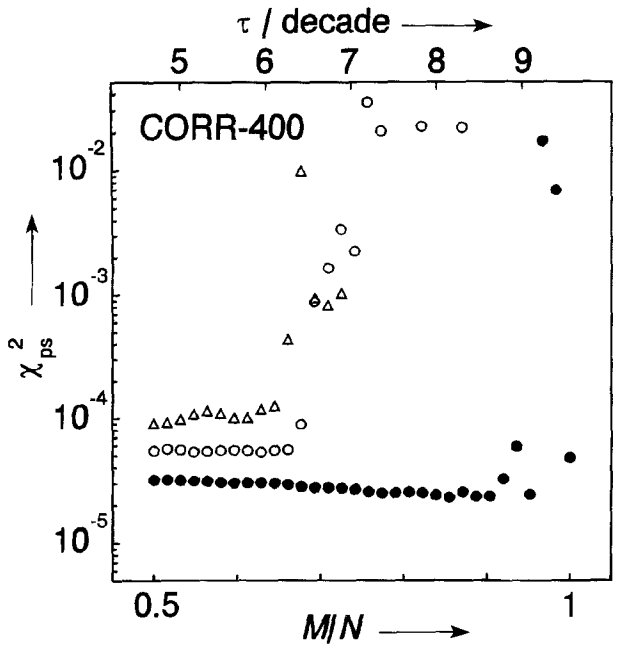

Fig. 18. Influence of the *M/N* ratio on χ^2_{ps} in the weighted fit procedures applied to the CORR-400 data: (●) for the complex fit, Eq. 19; (△) for the weighted real part fit with imaginary adjustment; (○) for the weighted imaginary part fit. The top axis represents the resulting number of Tcs per decade.

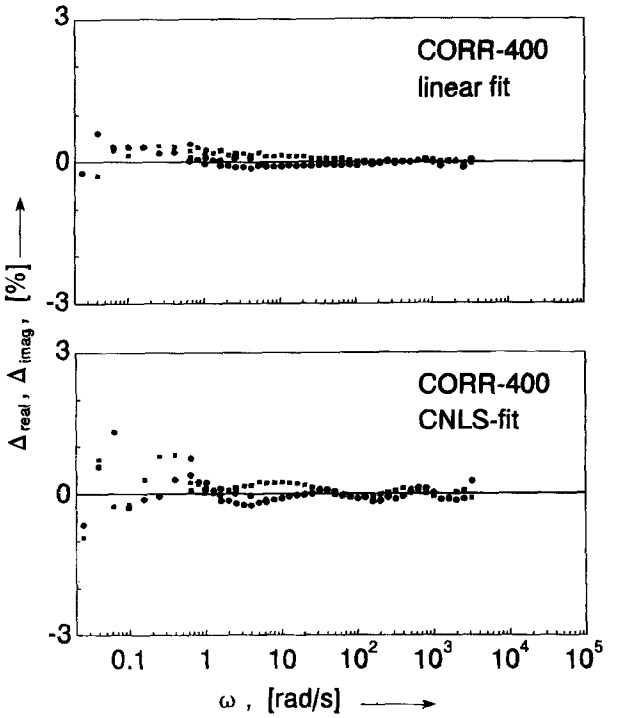

Fig. 20. Relative residuals for the reduced CORR-400 data set (ω values above 3000 rad/s excluded), (a, top) for the complex linear fit and (b, bottom) CNLS-fit using an EqC as presented in Ref. 25-27.

was investigated. The results are presented in Fig. 18. It is obvious that the number of Tcs per decade is quite crucial for the partial fit and transform procedures, giving a reasonable result for about five to six τ values per decade. As noticed before, the complex linear fit is much less affected, yielding acceptable results for nine or less τ values per decade.

The result of the complex linear fit for $M = 50$ (~7.6 τ values per decade) is presented in the residuals plot of Fig. 19. The shift in the position of the residuals above $\omega = 3000$ rad/s indicates a serious flaw in the data set. This has already been observed in a previous Kronig-Kramers data validation procedure of the CORR-400 data set, in which the procedure, as outlined in Ref. 15, was followed (unpublished results). Inspection of the dispersion in the impedance representation, Fig. 17b, shows that these high frequency data sets can be removed without a significant loss in information.

A subsequent analysis, in which data points above $\omega = 3000$ rad/s were excluded, gave a much improved result with $\chi^2_{ps} = 5.2 \times 10^{-6}$ *vs.* 2.6×10^{-5} for the full data set. The residuals plot is presented in Fig. 20a. Here a slight trace in both the real and imaginary parts is noticeable. This is not surprising as we are dealing here with a corroding system,

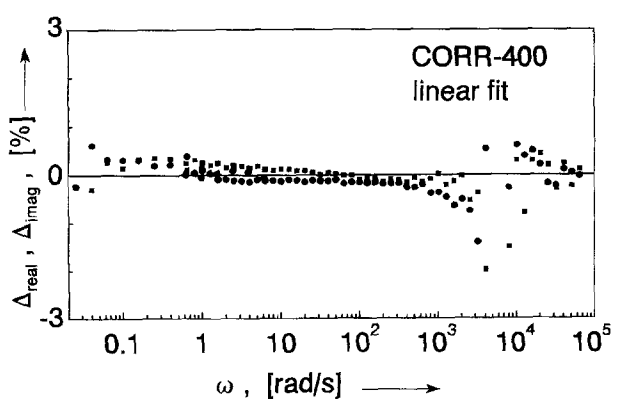

Fig. 19. Relative residuals for the complex linear fit of the CORR-400 data set with *M* = 50 (~7.6 τ values/decade).

which cannot be expected to be invariant for a prolonged time. The increased deviation for $\omega < 0.8$ rad/s is most likely due to the multisine fast Fourier transform (FFT) measuring technique, which was used at low frequencies. This becomes even more evident from the residuals plot for the CNLS-fit of the reduced data set (Fig. 20b), which also indicates that the applied EqC is probably too ideal.

Discussion and Conclusions

The linear fit and transform procedure presented here shows some similarities with respect to the inversion of dielectric relaxation spectra presented in Ref. 18, 19. A significant difference is that the inversion problem cannot allow negative probabilities (∝ fit parameters) for the τ_ks of distribution of time constants. For these problems a nonlinear fit procedure in which the τ_ks are left free, as recently described by Macdonald,[28] is more appropriate. For the K-K transform testing, the sign of the fit parameters is irrelevant as here the goal is to obtain a close fit to the (partial-) data set with the K-K transformability as imposed restriction. The applicability of the linear K-K testing is clearly demonstrated by the presented results, which were obtained for a very diverse set of immittance data. From these tests the picture emerges that the complex linear fit is quite robust with respect to the choice of the distribution and range of τ values. Through inspection of the relative residuals plots for these complex linear fits, it is possible to isolate data that do not comply with the K-K transformation rules, or to indicate which part of the frequency dispersion of the data set is questionable.

The single fit and transformation procedure, which in many instances could replace the K-K transform integrals (Eq. 2, 3), is quite sensitive to the choice of the parameter set size and even more so to the τ range. It is obvious that the reliability of the transformation strongly depends on the frequency range as well as on the number of overlapping dispersion sources in the electrochemical system. This is particularly true for the real to imaginary transformation. But, if substantial errors in the end regions of the dispersion are tolerable, again a simple, general, and fast K-K transformation is possible.

The additional fit of an inductance and a capacitance to the transformed imaginary data must be viewed more as a mathematical improvement, rather than having these elements "physically" present in the possible equivalent circuit model. This adjustment follows from the inadequacy of the model function to predict accurately the real part dispersion outside the frequency range of the measured data (as has been indicated in the section on the Basic Principle of the Linear Fit).

As a rule of thumb we can conclude that, for the single fit and transformation, the τ range should be equal to the inverse ω range with a distribution of 6 or 7 Tcs per decade. More field testing will be necessary, however, to obtain a clear understanding. With respect to the linear testing procedure in other immittance representations, the formulas can simply be derived from the equations presented here. For example a complex linear fit in the dielectric representation is obtained by dividing Eq. 19 by $j\omega C_0$, where C_0 is the capacitance of the empty cell

$$\epsilon(\omega_i) = C'_1 + \sum_{k=2}^{M-1} \frac{C'_k}{1 + (\omega_i\tau_k)^2} - j\left[\sum_{k=2}^{M-1} \frac{C'_k\omega_i\tau_k}{1 + (\omega_i\tau_k)^2} + \frac{C'_M}{\omega_i}\right] \quad [20]$$

with C'_k and C_k/C_0 and $C'_M = (R_0C_0)^{-1}$, and the parallel inductance omitted.

The main advantage of these linear fit/transform procedures is that no initial guesses are required. As there is no iterative convergence procedure, calculation times can be short (under 5 s for a data set of 65 frequencies and 50 parameters, using a personal computer with a 66 MHz 80486-DX2 and double precision reals). Hence the linear complex fit procedure could be used as a "K-K compliance filter" directly after the measurement has been finished. With the latest version of LEVM,[29] it is in principle possible to perform all these suggested linear fit procedures and K-K transform tests.

A further advantage of this procedure over the CNLS-fit of a simple multi-*R*-*C* circuit is that no negative time constants can occur as these have been defined as positive quantities. The problem with a negative τ value is that then either the resistance or the capacitance is negative. This situation is not K-K compatible, and a CNLS fit which yields one or more negative τ values may mask nonK-K behavior in certain data sets. The major drawback of this linear approach is that there is not yet a theoretical basis with which the observed behavior can be explained. Also the parameter sets do not seem to have a direct connection with the physical dispersive processes. Hence no distribution of Tcs can be extracted, which is one of the advantages of the recently published modified multi-*R*-*C* CNLS-fit procedure.[17] Finally, it would be interesting to test the possibilities of data extrapolation using the linear complex fit. Especially for the determination of the corrosion resistance in corroding systems this would be valuable. Further tests in this direction will be performed, but for a "full" construction of the possible low frequency dispersion, the series capacitance in Eq. 11 must be omitted. It should be stressed here that the additional inductances and capacitances only have a meaning with respect to the fit within the frequency range of the data.

Acknowledgments

The author is much obliged to Dr. J. A. L. Dobbelaar (formerly at Delft University of Technology), Dr. H. W. Brinkman and Dr. B. A. van Hassel (both of the University of Twente) for kindly providing the experimental impedance spectra. Special thanks go to Professor J. R. Macdonald (University of North Carolina at Chapel Hill) for his critical review of the manuscript and the valuable suggestions made therein.

Manuscript submitted Nov. 16, 1994, revised manuscript received Jan. 27, 1995.

The University of Twente assisted in meeting the publication costs of this article.

REFERENCES

1. J. R. Macdonald and J. A. Garber, *This Journal,* **124,** 1022 (1977).
2. J. R. Macdonald, J. Schoonman, and A. P. Lehnen, *J. Electroanal. Chem.,* **131,** 77 (1982).
3. J. R. Macdonald and L. D. Potter, Jr., *Solid State Ionics,* **24,** 61 (1987).
4. J. R. Macdonald, *J. Appl. Phys.,* **65,** 4845 (1989).
5. J. R. Macdonald, *Electrochim. Acta,* **35,** 1483 (1990).
6. B. A. Boukamp, *Solid State Ionics,* **18/19,** 136 (1986).
7. B. A. Boukamp, *ibid.,* **20,** 31 (1986).
8. B. A. Boukamp, *Equivalent Circuit,* Internal Report CT89/214/128, University of Twente (1989).
9. K. Levenberg, *Quart. Appl. Math.,* **2,** 164 (1944).
10. D. W. Marquardt, *J. Soc. Ind. Appl. Math.,* **11,** 431 (1963).
11. R. de L. Kronig, *J. Opt. Soc. Am.,* **12,** 547 (1926).
12. H. A. Kramers, *Z. Phys.,* **30,** 521 (1929).
13. H. W. Bode, *Network Analysis and Feedback Amplifier Design,* Chap. 14, Van Nostrand, New York (1945).
14. M. Urquidi-Macdonald, S. Real, and D. D. Macdonald, *Electrochim. Acta,* **35,** 1559 (1990).
15. B. A. Boukamp, *Solid State Ionics,* **62,** 131 (1993).
16. P. Agarwal, M. E. Orazem, and L. H. Garcia-Rubio, *This Journal,* **139,** 1917 (1992).
17. B. A. Boukamp and J. R. Macdonald, *Solid State Ionics,* **74,** 85 (1994).
18. D. R. Uhlman and R. M. Hakim, *J. Phys. Chem. Sol.,* **32,** 2652 (1971).
19. F. D. Morgan and P. D. Lesmes, *J. Chem. Phys.,* **100,** 671 (1994).
20. W. H. Press, B. P. Flannery, S. A. Teukolsky, and W. Y. Vettering, *Numerical Recipes,* p. 24, Cambridge University Press, Cambridge (1986).
21. P. Zoltowski, *J. Electronal. Chem.,* **178,** 11 (1984).
22. J. R. Macdonald, A. Hooper, and A. P. Lehnen, *Solid State Ionics,* **6,** 65 (1982).
23. J. R. Macdonald, *ibid.,* **58,** 97 (1992).
24. G. Láng, L. Kocsis, and G. Inzelt, *Electrochim. Acta,* **38,** 1047 (1993).
25. J. A. L. Dobbelaar, Ph.D. Thesis, Chap. 4, p. 59, Delft University of Technology (1990).
26. J. A. L. Dobbelaar and J. H. de Wit, *This Journal,* **137,** 2038 (1990).
27. B. A. Boukamp, in *Proceedings of 9th European Congress on Corrosion,* FU-252, Royal Netherlands Industries Fair (1989).
28. J. R. Macdonald, *J. Chem. Phys.,* Submitted.
29. J. R. Macdonald, CNLS software package 'LEVM', version 6.1 (1994).